

See discussions, stats, and author profiles for this publication at: <https://www.researchgate.net/publication/231239265>

Triphenylamine–Oligothiophene Conjugated Systems as Organic Semiconductors for Opto-Electronics

ARTICLE *in* CHEMISTRY OF MATERIALS · APRIL 2006

Impact Factor: 8.35 · DOI: 10.1021/cm060257h

CITATIONS

114

READS

52

6 AUTHORS, INCLUDING:



Pierre Frère

University of Angers

130 PUBLICATIONS 3,340 CITATIONS

SEE PROFILE



Jean Roncali

French National Centre for Scientific Research

349 PUBLICATIONS 14,630 CITATIONS

SEE PROFILE

Triphenylamine–Oligothiophene Conjugated Systems as Organic Semiconductors for Opto-Electronics

Antonio Cravino,* Sophie Roquet, Olivier Alévêque, Philippe Leriche, Pierre Frère, and Jean Roncali*

Group Linear Conjugated Systems, CIMMA, CNRS UMR 6200, University of Angers, 2, Bd. Lavoisier, 49045 Angers CEDEX, France

Received February 2, 2006. Revised Manuscript Received March 8, 2006

Two novel “hybrid” systems consisting of a triphenylamine core carrying π -conjugated terthienyl branches have been synthesized and characterized by differential scanning calorimetry, X-ray diffraction, cyclic voltammetry, UV–vis absorption, and fluorescence spectroscopy. The semiconductor potentialities of these compounds, which lead to glassy or amorphous films, have been evaluated by their implementation in very simple prototype devices that display electroluminescence at low voltage as well as a photovoltaic effect. Moreover, field-effect transistors based on one of these novel molecules display a high hole mobility ($1.1 \times 10^{-2} \text{ cm V}^{-1} \text{ s}^{-1}$). These results suggest that molecules leading to amorphous materials could represent a valid alternative as compared to systems that require control of the molecular orientation/organization.

Introduction

Organic semiconductors (OSCs) based on π -conjugated systems are of growing scientific and technological importance in the emerging field of “plastic” electronics. Associated with substrates such as paper, polymers, or textiles, these materials are paving the way toward light-weight and cost-effective flexible opto-electronic devices.^{1–8} Although each kind of device involved in soft opto-electronics requires the synthesis of active materials specifically designed to ensure functions such as light emission or light harvesting, charge transport generally represents a major limitation to the final output performance.

In this context, the low dimensionality of charge transport represents a major source of problems. Widely investigated p-type OSCs, such as oligothiophenes (nTs), may reach hole field-effect mobility exceeding that of amorphous silicon.^{9,10} However, these excellent performances can be obtained only by an accurate control of parameters such as interdistance and relative orientation of the conjugated molecules. Thus,

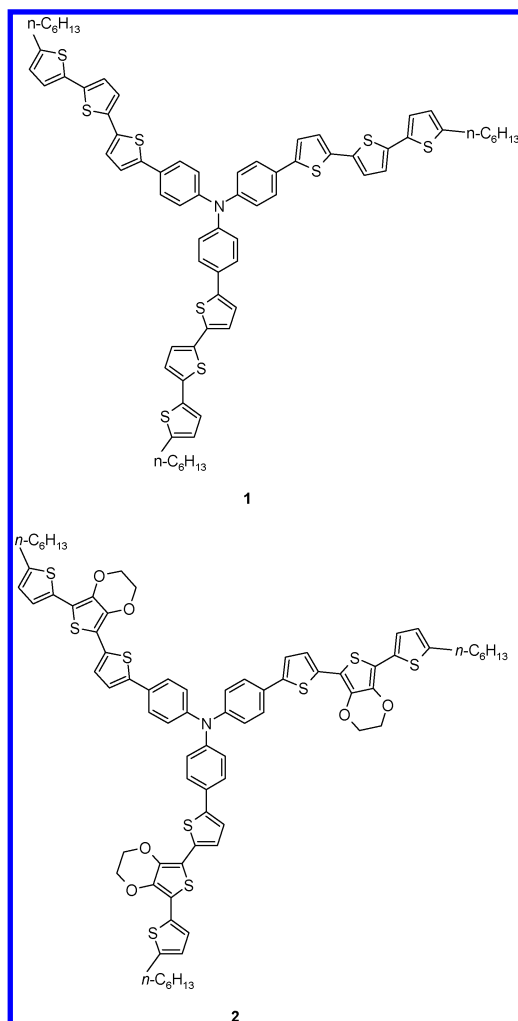
it has been shown that a vertical orientation of conjugated molecules on the substrate allows optimal charge transport across the channel of field-effect transistors (FETs) and, therefore, high charge-carrier mobility.^{1,2,6,10} However, such an orientation is deleterious for solar cells as it strongly limits the absorption of the incident light as well as the charge transport across the cell thickness.^{7,11} In other words, the control of molecular orientation represents a key issue for the achievement of optimal performance of organic devices based on low dimensional conjugated systems. In the case of low molecular mass materials the control of molecular order relies essentially on the optimization of the thermal deposition procedures, whereas for conjugated polymers, post-production thermal treatment is widely used to improve crystallinity and, hence, charge mobility.^{12–16} In each case, the search for ordered structures resembling as much as possible the ideal situation represented by single crystal OSCs is, explicitly or implicitly, the underlying concept.

A different possible approach would consist of the development of new classes of OSCs possessing anisotropic optical and charge transport properties. As a first step in this direction we have recently shown that tetrahedral architectures involving four oligothiophene chains attached to a silicon node represent interesting donor materials in bulk hetero-junction solar cells.¹⁷

* To whom correspondence should be addressed. E-mail: antonio.cravino@univ-angers.fr (A.C.); jean.roncali@univ-angers.fr (J.R.).

- (1) Dimitrakopoulos, C. D.; Malenfant, P. *Adv. Mater.* **2002**, *14*, 99.
- (2) Horowitz, G. *Adv. Funct. Mater.* **2003**, *13*, 53.
- (3) Kraft, A.; Grimsdale, A. C.; Holmes, A. B. *Angew. Chem., Int. Ed.* **1998**, *37*, 402.
- (4) Mitschke, U.; Baeuerle, P. *J. Mater. Chem.* **2000**, *10*, 1471.
- (5) Brabec, C. J.; Sariciftci, N. S.; Hummelen, J. C. *Adv. Funct. Mater.* **2001**, *11*, 15.
- (6) Garnier, F.; Yassar, A.; Hajlaoui, R.; Horowitz, G.; Deloffre, F.; Servet, B.; Ries, S.; Alnot, P. *J. Am. Chem. Soc.* **1993**, *115*, 8716.
- (7) Vidolot, C.; El Kassmi, A.; Fichou, D. *Sol. Energy Mater. Sol. Cells* **2000**, *63*, 69.
- (8) Burroughes, J. H.; Bradley, D. D. C.; Brown, A. R.; Marks, R. N.; Mackay, K.; Friend, R. H.; Burns, P. L.; Holmes, A. B. *Nature* **1990**, *347*, 539.
- (9) Sheraw, C. D.; Zhou, L.; Huang, J. R.; Gundlach, D. J.; Jackson, T. N.; Kane, M. G.; Hill, I. G.; Hammond, M. S.; Campi, J.; Greening, B. K.; Francl, J.; West, J. *Appl. Phys. Lett.* **2002**, *80*, 1088.
- (10) Halik, M.; Klauk, H.; Zschieschang, U.; Schmid, G.; Ponomarenko, S.; Kirchmeyer, S.; Weber, W. *Adv. Mater.* **2003**, *15*, 917.

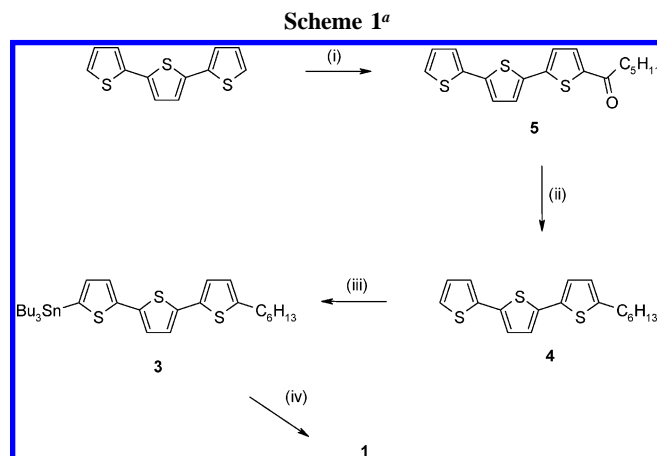
- (11) de Bettignies, R.; Nicolas, Y.; Blanchard, P.; Levillain, E.; Nunzi, J.-M.; Roncali, J. *Adv. Mater.* **2003**, *15*, 1939.
- (12) Padinger, F.; Rittberger, R.; Sariciftci, N. S. *Adv. Funct. Mater.* **2003**, *13*, 85.
- (13) Camaioni, N.; Ridolfi, G.; Casalbore-Miceli, G.; Possamai, G.; Maggini, M. *Adv. Mater.* **2002**, *14*, 1735.
- (14) Kim, Y.; Choulis, S. A.; Nelson, J.; Bradley, D. D. C.; Cook, S.; Durrant, J. R. *J. Mater. Sci.* **2005**, *40*, 1371.
- (15) Li, G.; Shrotriya, V.; Huang, J.; Yao, Y.; Moriarty, T.; Emery, K.; Yang, Y. *Nat. Mater.* **2005**, *4*, 864.
- (16) Ma, W.; Yang, C.; Gong, X.; Lee, K.; Heeger, A. J. *Adv. Funct. Mater.* **2005**, *15*, 1617.



Triphenylamine (TPA) derivatives are well-known and widely used as glass-forming and hole-injecting/transporting materials for organic light-emitting diodes (LEDs).^{18,19} Molecules consisting of a TPA core substituted by conjugated chains such as nTs, 2-phenylthiophene, or fluorene have been also reported. More recently, some first examples of organic FETs or solar cells based on molecules containing TPA blocks have been proposed and described, but the reported performances in terms of field-effect hole mobility (7×10^{-5} to $3 \times 10^{-4} \text{ cm}^2 \text{ V}^{-1} \text{ s}^{-1}$) or power conversion efficiency remain limited.^{19–22}

We report here the synthesis of compounds **1** and **2**, consisting in a TPA core derivatized with a terthienyl chain (**1**) and a thiophene–3,4-ethylenedioxythiophene (EDOT)–thiophene, (TET) motif (**2**).

The physical and electronic properties of these two compounds have been studied by differential scanning calorimetry (DSC), cyclic voltammetry, UV–vis absorption,



^a Reagents and conditions: (i) hexanoic anhydride, SnCl_4 , CH_2Cl_2 , 5 h; (ii) AlCl_3 , LiAlH_4 , Et_2O , 1 h and 30 min; (iii) *n*-butyllithium, THF, -60°C , 30 min, then Bu_3SnCl ; 30 min; (iv) tris(4-bromophenyl)amine, toluene, $\text{Pd}(\text{PPh}_3)_4$, reflux, 15 h.

and fluorescence spectroscopy. These molecules allow for the “wet” preparation of amorphous thin films. Simple devices that show some photovoltaic (PV) effects as well as electroluminescence (EL) at low voltage were prepared. In addition, molecule **1** shows an interesting FET mobility.

Results and Discussion

Synthesis. End-capped conjugated branches were prepared following two different strategies. The branch **4** (TTT) has been synthesized in a way similar to that reported in ref 23. Application of a homemade optimized process led to the target compound in 80% overall yield (Scheme 1).

The TET branch **7** was synthesized following a procedure similar to that described in ref 24 and then treated with butyllithium and tributyltin chloride to obtain the stannyl derivative **6** (Scheme 2).

The target compounds **1** and **2** were synthesized, in 65 and 45% yields, respectively, by Stille’s coupling reaction using the stannyl derivative of the corresponding conjugated branches and commercially available tris(4-bromophenyl)–amine.

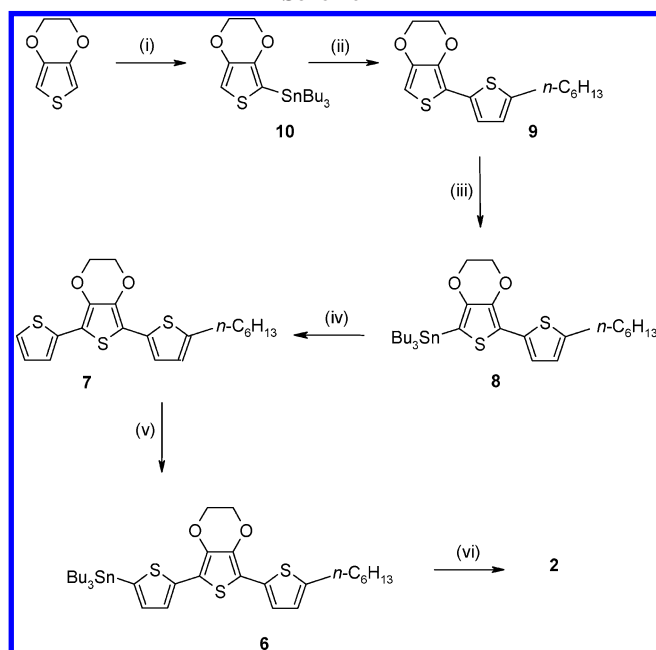
The molecules are soluble in solvents such as CH_2Cl_2 , chloroform, chlorobenzene, and toluene.

Thermal Analyses and X-ray Diffraction Studies. The thermal properties of **1** and **2** have been analyzed by DSC. The DSC trace of **1** shows the melting at each repeated scan. In the case of **2**, as displayed in Figure 1, the first DSC trace shows the melting peak around 140°C . However, upon cooling and subsequent heating, an endothermic peak characteristic of a glass transition is observed at about 80°C . X-ray diffraction experiments were performed both on **1** and **2** sampled as powder as well as spun-cast or evaporated thin films. In all cases, no reflection peaks were observed, indicating an amorphous character also for molecule **1**.

Cyclic Voltammetry. Figure 2 shows the cyclic voltammograms of compounds **1** and **2** in CH_2Cl_2 in the presence

- (17) Roncali, J.; Frère, P.; Blanchard, P.; de Bettignies, R.; Turbiez, M.; Roquet, S.; Leriche, P.; Nicolas, Y. *Thin Solid Films* [published online 18 January 2006, doi:10.1016/j.tsf.2005.12.01].
- (18) Shirota, Y. *J. Mater. Chem.* **2000**, *10*, 1.
- (19) Shirota, Y. *J. Mater. Chem.* **2005**, *15*, 75.
- (20) Saragi, T. P. I.; Fuhrmann-Lieker, T.; Salbeck, J. *Synth. Met.* **2005**, *148*, 267.
- (21) Sonntag, M.; Kreger, K.; Hanft, D.; Strohrriegel, P.; Setayesh, S.; de Leeuw, D. *Chem. Mater.* **2005**, *17*, 3031.
- (22) Petrella, A.; Cremer, J.; De Cola, L.; Bäuerle, P.; Williams, R. M. *J. Phys. Chem. A* **2005**, *109*, 11687.

- (23) Katz, H. E.; Dodabalapur, A.; Torsi, L.; Elder, D. *Chem. Mater.* **1995**, *7*, 2238.
- (24) Turbiez, M.; Frère, P.; Allain, M.; Vidélot, C.; Ackermann, J.; Roncali, J. *Chem.–Eur. J.* **2005**, *11*, 3742.

Scheme 2^b

^b Reagents and conditions: (i) *n*-butyllithium, THF, $-60\text{ }^{\circ}\text{C}$, then Bu_3SnCl ; (ii) 2-bromo-5-hexylthiophene, toluene, $\text{Pd}(\text{PPh}_3)_4$, reflux; (iii) *n*-butyllithium, THF, $-60\text{ }^{\circ}\text{C}$, then Bu_3SnCl ; (iv) 2-bromothiophene, toluene, $\text{Pd}(\text{PPh}_3)_4$, reflux; (v) *n*-butyllithium, THF, $-60\text{ }^{\circ}\text{C}$, then Bu_3SnCl ; (vi) tris(4-bromophenyl)amine, toluene, $\text{Pd}(\text{PPh}_3)_4$, reflux, 15 h.

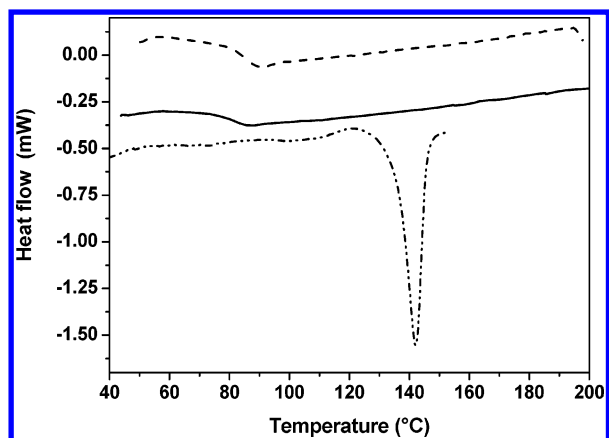


Figure 1. DSC traces (offset introduced for clarity) of **2**. Dotted-dashed line, first scan at $10\text{ }^{\circ}\text{C}/\text{min}$; dashed line, second scan at $10\text{ }^{\circ}\text{C}/\text{min}$; and solid line, third scan at $20\text{ }^{\circ}\text{C}/\text{min}$.

of tetrabutylammonium hexafluorophosphate. Both compounds undergo a reversible oxidation process indicative of stable radical cations. The redox potential E° for **1** is at 0.53 V (versus Ag/AgCl), while for **2** it is found at 0.47 V. The lower E° value found for **2** reflects the electron donating effect of the median EDOT ring.

UV–Vis Absorption and Fluorescence Spectroscopy.

Figure 3 shows the UV–vis absorption and fluorescence emission spectra of compounds **1** and **2** in CH_2Cl_2 . The spectrum of compound **1** displays an absorption maximum (λ_{max}) at 429 nm (2.89 eV). The spectrum of compound **2** shows a maximum at 439 nm (2.82 eV) and a shoulder at 460 nm (2.7 eV). The 10 nm red shift of λ_{max} between compounds **1** and **2** is due to the electron-donor effect of the EDOT unit, in agreement with the cyclic voltammetry data.

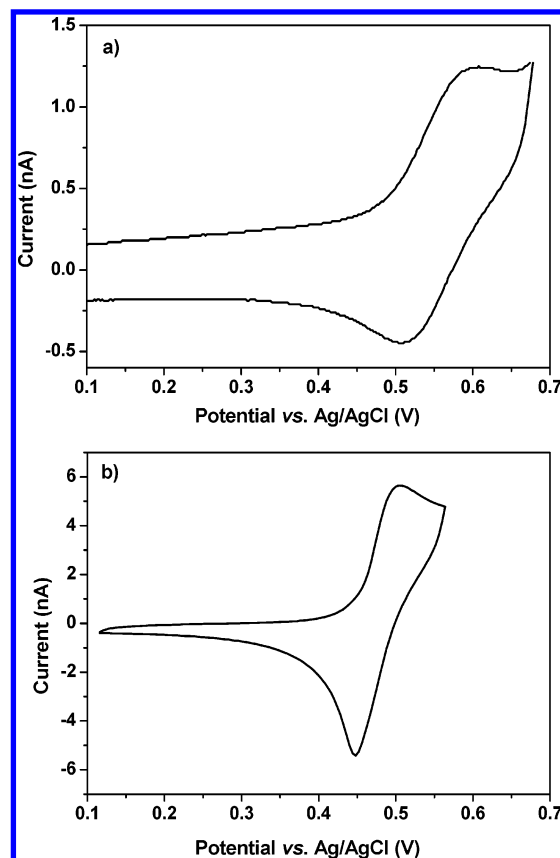


Figure 2. Cyclic voltammograms of **1** (a) ($1.5 \times 10^{-4}\text{ mol L}^{-1}$) and **2** (b) ($4.4 \times 10^{-4}\text{ mol L}^{-1}$) in 0.10 M $\text{Bu}_4\text{NPF}_6/\text{CH}_2\text{Cl}_2$, scan rate 100 mV s^{-1} .

The shoulder observed in the spectrum of **2** suggests a rigidification of the conjugated branches by intramolecular sulfur–oxygen interactions as already reported for many EDOT containing systems.²⁵

Compound **1** presents an unresolved fluorescence emission spectrum with maximum at 500 nm, whereas **2** shows a maximum at 496 nm and a shoulder at 523 nm. The two compounds show fluorescence emission quantum yields of 0.22 and 0.17, respectively (using anthracene as a standard). As already observed for hybrid systems combining nTs and TPA,²⁶ these quantum yields are significantly higher than the value (0.06) found for the constitutive building blocks, TPA,²⁶ TTT, and TET.²⁴

Realization and Evaluation of Thin Film Devices. The fact that compound **2** retains a photoluminescence (PL) detectable by the eyes in thin films cast from solution, together with the electrical characteristics found for indium tin oxide (ITO)/Baytron P/Al diodes (Ohmic contacts, see Supporting Information), led us to consider investigating them as possible electroluminescent devices. Indeed, simple diodes consisting of a single layer of compound **2** spun-cast from chlorobenzene solution onto a Baytron P pretreated ITO electrode and completed by thermal evaporation of an aluminum cathode were functioning LEDs.

Figure 4 shows the EL spectrum of the devices, along with the electronic absorption spectrum of a spun-cast film of

(25) Turbiez, M.; Frère, P.; Allain, M.; Gallego-Planas, N.; Roncali, J. *Macromolecules* **2005**, *38*, 6806.

(26) Noda, T.; Nogawa, N.; Noma, N.; Shirota, Y. *J. Mater. Chem.* **1999**, *9*, 2177.

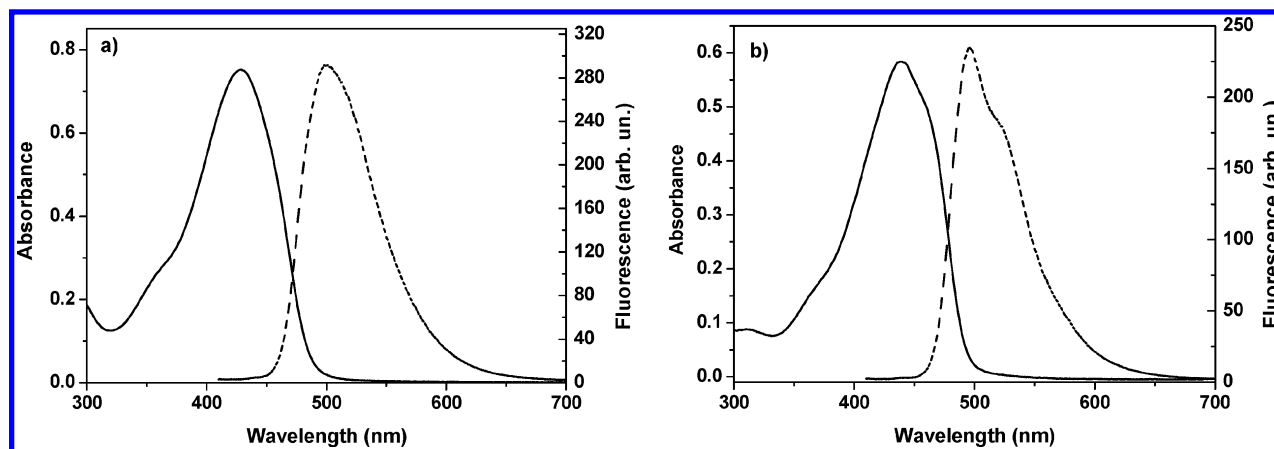


Figure 3. UV-vis absorption (solid) and fluorescence emission (dashed) spectra of **1** (a) and **2** (b) in CH_2Cl_2 .

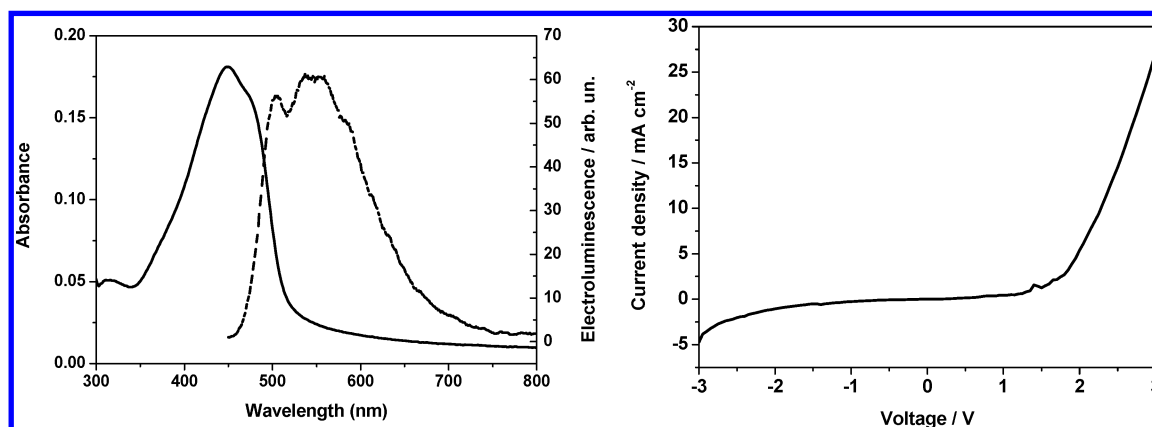


Figure 4. Left: EL spectrum of ITO/Baytron/2/Al devices (dotted line) and electronic absorption of a spun-cast (chlorobenzene) film of **2** (solid line). Right: current vs voltage curve of ITO/Baytron/2/Al devices.

compound **2**. As a result of intermolecular interactions in the solid state, both spectra exhibit an about 10 nm red shift as compared to those recorded in solution. The typical current density/voltage (J/V) curve of the devices is also depicted in Figure 4. A qualitative characterization of the devices is given in Supporting Information.

As can be seen in Figure 4, the turn-on voltage values were in the range 1.9–3 V. Typically, the emitted green light was already detectable by the naked eye around 2 V. These low values suggest that compound **2** possesses good hole injecting properties and that the concepts underlying the synthesis of **2** may be extended to the design of active compounds with dual charge-injecting/transport and light-emitting properties for application in LEDs.

The potentialities of compounds **1** and **2** as donor material in PV devices have been evaluated in bilayer heterojunctions using fullerene C_{60} as the electron acceptor. The cells were realized by spin-casting a film of donor from a chlorobenzene solution onto an ITO-coated glass electrode precoated with a film of Baytron P. A layer of fullerene C_{60} was then deposited by sublimation under high vacuum, and the cell was completed by thermal evaporation of aluminum as the top electrode (see Experimental Section for details).

Figure 5 shows the current density voltage (J/V) characteristics of the cells based on the two donors. At ± 1 V, the devices do not behave as diodes. The current onset is seen above 1 V (not shown), as observed for the single layer devices. Under illumination a clear PV effect is established,

suggesting the occurrence of a photoinduced electron transfer from **1** and **2** to C_{60} . Under 100 mW cm^{-2} simulated AM1.5 solar illumination, the devices deliver a short circuit current density (J_{SC}) of 1.7 and 1.5 mA cm^{-2} , for donors **1** and **2**, respectively.

The cells based on donor **1** deliver an open-circuit voltage (V_{OC}) of 0.67 V while this value falls to 0.32 V for donor **2**. This difference is in qualitative agreement with the lower oxidation potential of donor **2**.^{27,28} The efficiency of the cells is essentially limited by the low value of the filling factor (FF), only about 0.3. This latter characteristic, known to be the most critical for organic PV devices,²⁹ limits the power conversion efficiency³⁰ to 0.32% for **1** and 0.14% for **2**.

In addition, TPA derivatives are well-known for their photoconductivity. Although photoconductivity might improve charge-carrier transport, its occurrence might be deleterious for the FF as well as the V_{OC} values. For a better understanding of the device's behavior, further studies of the contact between ITO/Baytron and **1** or **2** in the dark and especially under illumination, as well as of the intrinsic photoconductive properties of the molecules, are necessary.

(27) Brabec, C. J.; Cravino, A.; Meissner, D.; Sariciftci, N. S.; Fromherz, T.; Rispens, M. T.; Sanchez, L.; Hummelen, J. C. *Adv. Funct. Mater.* **2001**, *11*, 374.

(28) Gadisa, A.; Svensson, M.; Andersson, M. R.; Inganäs, O. *Appl. Phys. Lett.* **2004**, *84*, 1609.

(29) Rostalski, J.; Meissner, D. *Sol. Energy Mater. Sol. Cells* **2000**, *61*, 87.

(30) Calculated as $\eta = J_{\text{SC}}V_{\text{OC}}\text{FF}/P_{\text{in}}$, where $\text{FF} = J_{\text{mpp}}V_{\text{mpp}}/J_{\text{SC}}V_{\text{OC}}$.

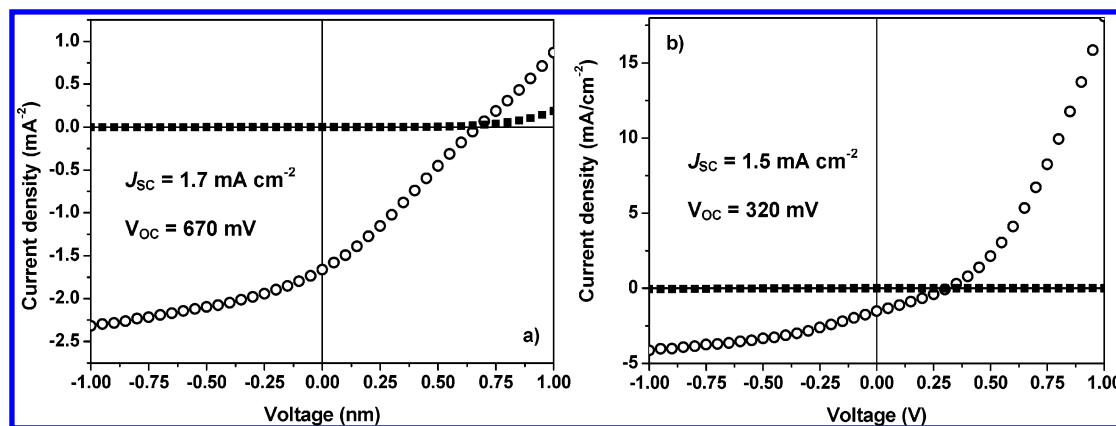


Figure 5. J/V curves of ITO/Baytron/1/C₆₀/Al (a) and ITO/Baytron/2/C₆₀/Al (b) thin film devices. Black squares: dark. Open circles: simulated AM1.5 100 mW cm⁻² illumination.

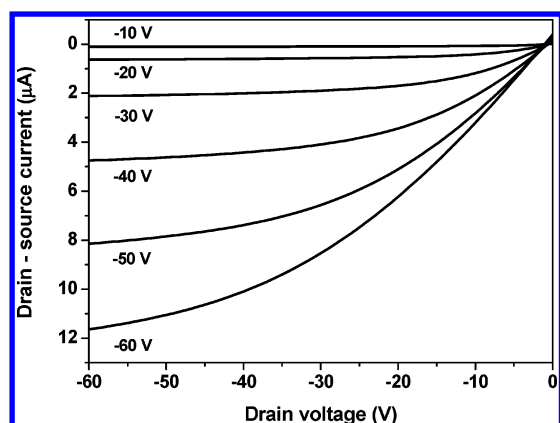


Figure 6. I_{SD}/V_{SD} curves at different V_G values for FETs based on an evaporated layer of **1**.

Although limited by the above-discussed factors, the PV efficiency of these devices compares very well with that of analogous cells based on a number of p-type conjugated polymers and oligomers or flat OSCs, even when the latter were thermally evaporated and *better matching* the solar spectrum. As recent examples, for evaporated bilayer devices consisting of a sexithiophene derivative or zinc phthalocyanine as the donor and C₆₀ as the acceptor, AM1.5 efficiencies of 0.12–0.13% have been reported.^{31,32}

The above results suggest that amorphous materials such as compounds **1** and **2** might be efficient hole-transporting materials. To confirm this point, thin film FETs have been realized using heavily doped silicon as the gate, SiO₂ as the dielectric layer, and Au as the top contact source and drain electrodes. Devices prepared by spin coating **1** or **2** showed field-effect hole mobility values around 10⁻⁵ cm² V⁻¹ s⁻¹. However, the evaporation of **1** allowed for the attainment of reproducible sets of devices that display dramatically higher mobility. Because the material has been found amorphous independent of the deposition technique, a possible explanation for the higher mobility measured in evaporated films might be a more dense structure, not attainable by spin-casting, beneficial for intermolecular contacts.

Figure 6 shows the source–drain current/source–drain voltage (I_{SD}/V_{SD}) curves of the latter devices at different gate

voltages (V_G). The curves display a clear FET behavior. The threshold voltage was found between -18 and -20 V. Field-effect mobility, calculated from the saturation regime of I_{SD} ,³³ reaches values up to 1.1 × 10⁻² cm² V⁻¹ s⁻¹. Whereas comparable values have been recently measured by the time-of-flight technique for tri(oligoarylenyl)amines,³⁴ to the best of our knowledge these results represent the highest FET hole mobility reported so far for a TPA-based material. However, a low on/off ratio (170–200) clearly shows that the FET devices need to be optimized.

Conclusion

Two novel TPA–oligothiophene hybrid systems have been synthesized. These molecules lead to amorphous materials which have been implemented in very simple thin film LEDs, hetero-junction solar cells, and FETs. The preliminary results obtained seem encouraging especially when considering that, contrary to polycrystalline or polymeric OSCs, amorphous TPA based materials do not require control of molecular orientation. Work aiming at the development of other members of this class of compounds by varying the length and composition of the conjugated chains is now underway and will be reported in future publications.

Experimental Section

General Methods. Thin film chromatography was done on silica 60F₂₅₄ or neutral alumina F₂₅₄ (Merck) plates. For column chromatography, the stationary phase was silica 60F (35–70 μm, SDS). Solvents were purified and dried using standard protocols. Melting points were taken by a K f ler plate or by a microscope Reichert-Thermovar and are uncorrected. NMR spectra were taken by a Bruker AVANCE DRX 500 (¹H, 500 MHz; ¹³C 125, 7 MHz) spectrometer. Chemical shifts are given as δ (ppm) versus tetramethylsilane as the internal standard. matrix-assisted laser desorption/ionization time-of-flight (MALDI-TOF) mass spectra were recorded by a Bruker Biflex-III, equipped with a N₂ laser (337 nm). For the matrix, dithranol in CH₂Cl₂ was used.

Thermal analyses were performed using a DSC 2010 CE (TA Instruments). X-ray (Cu α) diffraction experiments were carried out

(31) Mason, C. R.; Skabara, P. J.; Schofield, D. J.; Meghdadi, F.; Ebner, B.; Sariciftci, N. S. *J. Mater. Chem.* **2005**, *15*, 1446.
(32) Brousse, B.; Ratier, B.; Moliton, A. *Thin Solid Films* **2004**, *451*, 81.

(33) Sze, S. M. *Physics of Semiconductor Devices*; Wiley: New York, 1981; p 496.
(34) Ohishi, H.; Tanaka, M.; Kageyama, H.; Shirota, Y. *Chem. Lett.* **2005**, *33*, 1266.

working in θ – 2θ reflection mode using a Bruker D500 diffractometer equipped with a speed detector Vantec.

UV–vis absorption spectra were taken by a Lambda 19 (Perkin-Elmer) spectrophotometer. For cyclic voltammetry (scan rate 100 mV cm^{−1}), the electrochemical apparatus consisted of a potentiostat EG&G PAR 273A and of a standard three-electrode cell. As the working and counter electrodes, a platinum foil and a platinum wire were used, respectively, while as a reference a Ag/AgCl electrode was used.

Devices Preparation and Characterization. Fullerene C₆₀ (99+%) was purchased from Mer and used as received. The Baytron suspension used to apply smoothing and hole conducting/injecting layers was purchased as “Baytron P PE FL” (HC Stark). For spin-casting of **1** and **2**, HPLC grade chlorobenzene (Aldrich) was used. All thin film devices were prepared in laboratory conditions. As electrodes, ITO coated glasses (40 Ω/\square , Solem) and evaporated Al films (ca. 60 nm thick) were used. The ITO electrodes were cleaned in ultrasonic baths, subjected to an UV–ozone treatment (15 min), and then modified by a spun-cast layer of Baytron (60–80 nm thick), which was dried at 115 °C for 20 min. The Baytron suspension was stirred at about 70 °C and filtered through a 0.45 μ m membrane (Minisart RC 15, Sartorius) just prior to casting. A 60 nm thick layer of Al was thermally evaporated through a shadow mask, at a pressure of about 10^{−6} mbar. The mask geometry defined a device's area of 0.32 cm². Every plaque of ITO coated glass supported two individual devices. Different “sets” of devices, using the same batch and solution and whereon Al was evaporated simultaneously, were prepared. Thin films were cast by spin-coating solutions in chlorobenzene.

Devices with ITO/Baytron/**1** (or **2**)/Al structure were produced from solutions with a concentration of 10 mg mL^{−1}. Bilayer heterojunction devices (ITO/Baytron/**1** (or **2**)/C₆₀/Al) were fabricated by spin-coating, with a donor concentration of 5 mg mL^{−1}, followed by the thermal evaporation in a vacuum of a 20 nm thick layer of C₆₀. The thickness was controlled by an oscillating quartz monitor. For casting Baytron as well as the molecules, the spin-coating program was always as follows: an acceleration ramp (10 s) from 0 to 1500 rpm followed by a plateau (30 s) and a drying step at 2000 rpm (1 min). After preparation, the devices were stored and characterized in an argon glovebox (200B, MBraun). The *J*–*V* curves of the devices were recorded in the dark and under illumination using a Keithley 236 source-measure unit and a homemade acquisition program. The light source was an AM1.5 Solar Constant 575 PV simulator (Steuernagel Lichttechnik, equipped with a metal halogenide lamp). The light intensity was measured by a broad-band power meter (13PEM001, Melles Griot). The devices were illuminated through the ITO electrode side. The efficiency values reported here are not corrected, neither for the possible solar simulator spectral mismatch nor for the reflection/absorbance of the glass/ITO/Baytron coated electrodes. PL and EL spectra were recorded by a PTI Master fluorimeter. For EL measurements, the devices were wired in air by soldering indium. The wired devices were fixed into protective transparent boxes that were then transferred inside the glovebox. After 1 h in an argon atmosphere, the boxes were sealed by molten paraffin and used to record the EL spectra. For these latter experiments, the electrical source-measure unit was a potentiostat EG&G PAAR 273.

Organic FETs were prepared by evaporation of a 50 nm thick organic layer onto a Si n++ wafer with a 200 nm thick SiO₂ layer (ACM). As source and drain top contacts, 25 nm of Au were evaporated through a homemade shadow mask, defining a channel with 5000 μ m width and 60 μ m length. The characterization was carried out in the glovebox using an Agilent 4155C semiconductor

parameter analyzer. The contacts were obtained by W tips (Sig-natone).

3',4'-Ethylenedioxy-5''-hexyl-2-tributylstannyl-5,2':5',2''-terthiophene (6). In an inert atmosphere, a solution of **7** (1.61 g, 4.1 mmol) in anhydrous tetrahydrofuran (THF; 20 mL) was cooled to −60 °C, and then 2.5 M butyllithium in hexane (2.5 mL, 1.5 equiv) was added dropwise. The mixture was stirred at −60 °C for 30 min and then at −40 °C for 30 min. After cooling back to −60 °C, tributyltin chloride (2 mL) was added dropwise, and the temperature was allowed to rise to 25 °C. After dilution with diethyl ether, the organic phase was washed with saturated aqueous NH₄Cl and water and then concentrated. The residue was diluted in ethylacetate, added to saturated aqueous NaF, and stirred for 30 min. After filtration (hyflosuperpel) and decantation, the organic phase was dried over anhydrous MgSO₄. Filtration and evaporation of the solvent gave an oil that was used without further purification.

5-Hexanoyl-2,2':5',2''-terthiophene (5). Terthiophene (4.5 g, 16 mmol) was dissolved under an inert atmosphere in dichloromethane (45 mL) dried over P₂O₅. Hexanoic anhydride (4.23 mL, 1.1 equiv) was quickly added, and then 2.08 mL (1.1 equiv) of aqueous tin chloride was added dropwise in 15 min. The solution turned red and was stirred at room temperature for 5 h. The mixture was then poured over ice containing 27 mL of glacial acetic acid. After addition of dichloromethane, the organic phase was washed twice with 10% aqueous NaOH and then water. After drying over anhydrous magnesium sulfate, filtration, and solvent evaporation, the crude was purified by column chromatography (silica, petroleum ether/dichloromethane, 1:1). A total of 3.64 g (66%) of a brown solid, mp 133 °C, was obtained. ¹H NMR (CDCl₃) δ : 7.590 (1H, d, *J* = 3.60), 7.25 (1H, d, *J* = 5.10), 7.20 (2H, m), 7.15 (1H, d, *J* = 3.60), 7.11 (1H, d, *J* = 3.60), 7.04 (1H, dd, *J* = 5.10 and 3.60), 6.68 (1H, d, *J* = 3.50), 2.79 (2H, t, *J* = 7.70), 1.38 (2H, quint, *J* = 7.60), 1.31 (6H, m), 2.86 (2H, t, *J* = 7.70), 1.76 (2H, quint, *J* = 7.60), 1.36 (4H, m), 0.92 (3H, t, *J* = 6.90). IR (KBr) ν /cm^{−1}: 1657.

5-Hexyl-2,2':5',2''-terthiophene (4). Cooled by an ice bath, AlCl₃ (2.76 g) and LiAlH₄ (3.15 g, 8 equiv) in anhydrous ether (100 mL) were added to **5** (3.61 g, 0.5 equiv) partially dissolved in toluene (150 mL). The mixture was stirred at room temperature under a nitrogen atmosphere for 3 h and 30 min. Then ethyl acetate (25 mL) and 6 M HCl (30 mL) were added slowly, and the mixture was further stirred for 1 h and 30 min. After addition of water and phase separation, the aqueous phase was extracted by diethyl ether (2 \times 170 mL). The organic phase was washed with saturated aqueous Na₂CO₃ (150 mL) and then water and dried over anhydrous magnesium sulfate. Solvent evaporation and column chromatography (silica (slurry in petroleum ether), petroleum ether/dichloromethane, 2:1) gave 2.78 g (80%) of a yellow solid, mp 66 °C. ¹H NMR (CDCl₃) δ : 7.20 (1H, dd, *J* = 5.10 and 1.10), 7.15 (1H, dd, *J* = 3.80 and 1.10), 7.05 (1H, d, *J* = 3.80), 7.01 (1H, dd, *J* = 3.5 and 5.10 and 3.60), 6.99 (1H, d, *J* = 3.80), 6.98 (1H, d, *J* = 3.50), 6.68 (1H, d, *J* = 3.50), 2.79 (2H, t, *J* = 7.70), 1.38 (2H, quint, *J* = 7.60), 1.31 (6H, m), 0.89 (3H, t, *J* = 6.90).

5''-Hexyl-2-tributylstannio-5,2':5',2''-terthiophene (3). Compound **3** was prepared as described for **6**, using **4** (0.59 g, 1.8 mmol) in THF (15 mL), 1.6 M butyllithium in hexane (1.7 mL, 1.5 equiv), and tributyltin chloride (0.82 mL, 1.7 equiv). The reaction yielded 1.12 g of oil, which was used without purification.

Tris[4-(3',4'-ethylenedioxy-5''-hexyl-5-terthienyl)phenyl]amine (2). A total of 320 mg (0.67 mmol) of tris(4-bromophenyl)amine was dissolved in 30 mL of degassed toluene. To the solution were added **6** (3.17 g, 7 equiv) and Pd(PPh₃)₄ (40 mg). The mixture was kept under reflux for 15 h. After removal of toluene, the crude product was dissolved in 200 mL of dichloromethane, washed with

300 mL of water, and then dried over anhydrous magnesium sulfate. After filtration, the residue was washed with petroleum ether. The solid was filtered by a frit and then recrystallized from 1:1 petroleum ether/dichloromethane, to afford **2** (0.42 g, 45%) as a brown powder, mp 135 °C. ^1H NMR (CDCl_3) δ : 7.50 (2H, d, $J = 8.56$), 7.16 (2H, m), 7.12 (2H, d, $J = 8.33$), 7.03 (1H, d, $J = 3.5$), 6.69 (1H, d, $J = 3.51$), 4.39 (4H, m), 2.80 (2H, t, $J = 7.21$), 1.68 (2H, quint, $J = 7.35$), 1.38 (2H, m), 1.32 (4H, m), 0.89 (3H, t, $J = 6.67$). ^{13}C NMR (CDCl_3) δ : 146.2, 145.0, 141.9, 137.5, 136.9, 133.4, 131.7, 129.1, 126.4, 124.4, 124.2, 123.6, 122.7, 122.6, 110.1, 109.1, 65.0, 64.9, 31.6, 31.5, 30.1, 28.8, 22.6, 14.1. MS (MALDI-TOF) m/z : 1410 $[(\text{M} + \text{H})^+]$.

Tris[4-(5''-hexyl-5-terthienyl)phenyl]amine (1). Compound **1** was prepared as described for **2** using TPA (120 mg), toluene (12 mL), **3** (1.12 g), and $\text{Pd}(\text{PPh}_3)_4$ (20 mg). The crude was dissolved in dichloromethane and filtered. After removal of the solvent, 0.09 g of an orange solid were obtained. Further, 0.10 g of the same solid were recovered by washing the insoluble residue with

dichloromethane. Yield, 65%; mp 174 °C. ^1H NMR ($\text{CDCl}_3/\text{CS}_2$, 1:1) δ : 7.48 (2H, d, $J = 8.64$), 7.14 (2H, d, $J = 8.69$), 7.13 (1H, d, $J = 3.69$), 7.08 (1H, d, $J = 3.80$), 7.03 (1H, d, $J = 3.71$), 6.96 (1H, d, $J = 3.78$), 6.94 (1H, d, $J = 3.53$), 6.66 (1H, d, $J = 3.55$), 2.81 (2H, t, $J = 7.58$), 1.69 (2H, quint, $J = 7.50$), 1.35 (6H, m), 0.93 (3H, t). ^{13}C NMR ($\text{CDCl}_3/\text{CS}_2$, 1:1) δ : 146.1, 145.2, 142.5, 136.6, 135.9, 135.4, 134.4, 128.8, 126.5, 124.7, 124.3, 124.2, 123.9, 123.4, 123.3, 123.0, 31.7, 31.6, 30.2, 28.9, 22.3, 14.2. MS (MALDI-TOF) m/z : 1235.

Supporting Information Available: Discussion of electrical contact characteristics, including the J/V curve and logarithmic plot of the J/V curve of ITO/Baytron/2/Al thin film devices, EL discussion and spectra, and the electronic absorption of molecule **1** as a thin film (PDF). This material is available free of charge via the Internet at <http://pubs.acs.org>.

CM060257H